NANO LETTERS

Letter

pubs.acs.org/NanoLett

Intrinsic Two-Dimensional Organic Topological Insulators in Metal–Dicyanoanthracene Lattices

L. Z. Zhang,[†,‡,§] Z. F. Wang,[§,⊥] B. Huang,[§] B. Cui,[§] Zhiming Wang,[*,†] S. X. Du,[*,‡] H.-J. Gao,[‡] and Feng Liu[*,§,¶]

[†]Institute of Fundamental and Frontier Sciences, University of Electronic Science and Technology of China, Chengdu 610054, China

[‡]Institute of Physics, Chinese Academy of Sciences, Beijing 100190, China

[§]Department of Materials Science and Engineering, University of Utah, Salt Lake City, Utah 84112, United States

[⊥]Hefei National Laboratory for Physical Sciences at the Microscale and Synergetic Innovation Center of Quantum Information and Quantum Physics, University of Science and Technology of China, Hefei, Anhui 230026, China

[¶]Collaborative Innovation Center of Quantum Matter, Beijing 100084, China

Supporting Information

ABSTRACT: We predict theoretical existence of intrinsic two-dimensional organic topological insulator (OTI) states in Cu–dicyanoanthracene (DCA) lattice, a system that has also been grown experimentally on Cu substrate, based on first-principle density functional theory calculations. The p_z-orbital Kagome bands having a Dirac point lying exactly at the Fermi level are found in the freestanding Cu–DCA lattice. The tight-binding model analysis, the calculated Chern numbers, and the semi-infinite Dirac edge states within the spin–orbit coupling gaps all confirm its intrinsic topological properties. The intrinsic TI states are found to originate from a proper number of electrons filling of the hybridized bands from Cu atomic and DCA molecular orbitals based on which similar lattices containing noble metal atoms (Au and Cu) and those molecules with two CN groups (DCA and cyanogens) are all predicted to be intrinsic OTIs.

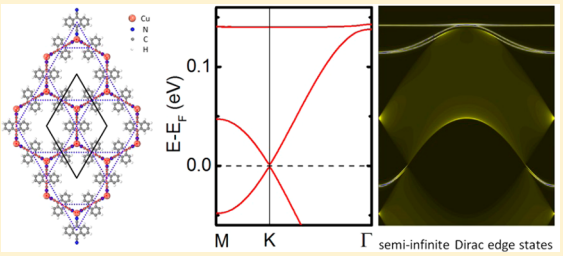

KEYWORDS: *Topological insulator, intrinsic, organometallic framework, Dirac band, flat band*

Two-dimensional (2D) topological insulators (TIs) exhibit quantum spin Hall (QSH) effect with spin-filtered edge states in the bulk gaps.[1−3] Besides the inorganic 2D TIs, with two material systems of HgTe/CdTe and InAs/GaSb/AlSb[4,5] being already experimentally confirmed, it recently has been predicted that organometallic lattices consist of an interesting class of 2D organic topological insulators (OTIs),[6] and subsequently more 2D OTIs are predicted and investigated.[7−16] The OTIs could be extremely important for the field of organic/molecular spintronics,[17−19] as they could expand the range of organic materials that can be used for spintronics applications.[8] Compared to the inorganic materials, organic materials have potentially the advantages of low cost, easy fabrications, and mechanical flexibility.

To date, two families of 2D OTIs have been investigated. The first group is made of hexagonal organometallic lattice in which metal atoms bond with three phenyl groups;[6−8] the second group is made of Kagome lattice in which metal atoms bond with two neighboring molecular groups.[9−16] Experimentally, none of the structures predicted in the first group has yet been made, while a few structures in the second group have been synthesized in the experiments.[9−12] However, none of the 2D OTIs[9−16] predicted in the second group with a Kagome lattice is intrinsic; hence, heavy doping (one or two electrons per unit cell) is required to move the Fermi level to inside the gap opened by spin–orbit coupling (SOC) at the Dirac point[13−16] before measurements of topological properties can be conducted.

It is important to realize that as a coordination polymeric material, organometallic (or metalorganic) lattices are usually formed according to specific electron counting rules of coordination chemistry. Consequently, nonisovalent doping, for example, substitution of the host metal atom with a foreign metal atom of different valence, which changes coordination chemistry, is usually difficult without changing the geometric structure. This is especially true for heavy doping up to the stoichiometric limit[20] with all the host metal atoms replaced, as required. Alternatively, doping of the organometallic (or metalorganic) lattices may be achieved by changing the oxidation states of the metal ions through redox control.[21] However, such a process is still limited by the amount of doping it can achieve; in general, it is highly desirable if intrinsic 2D OTIs can be found so that topological states can be realized and measured directly without doping.

Received: January 8, 2016
Revised: February 10, 2016
Published: February 11, 2016

DOI: 10.1021/acs.nanolett.6b00110
Nano Lett. 2016, 16, 2072–2075

In this Letter, we report the first intrinsic 2D OTI in an existing experimental synthesized system, the Kagome lattice of Cu−dicyanoanthracene (DCA),[22,23] based on first-principle density functional theory (DFT) calculations. The calculated Chern numbers and the semi-infinite Dirac edge states within the SOC gaps both confirm the nontrivial topological properties of this lattice. The single-orbital tight-binding (TB) model fitting to the DFT bands helps to further reveal the mechanism of the SOC gap opening. The intrinsic TI states are found to originate from a proper number of electrons filling the hybridized bands from Cu atomic and DCA molecular orbitals. On the basis of this finding, we further predict a number of similar intrinsic 2D OTIs.

All DFT calculations are carried out using Vienna ab initio simulation package (VASP)[24] with the projector augmented wave method, and a generalized gradient approximation (GGA) in the form of Perdew−Burke−Ernzerhof (PBE) is adopted for the exchange−correlation functional.[25] The energy cutoff of the plane-wave basis sets is 400 eV. A 5 × 5 × 1 Monkhorst−Park k-point mesh is used to do the static self-consistent calculation. In all the calculations, a 15 Å vacuum layer is used, and all atoms are fully relaxed until the residual forces on each atom are smaller than 0.01 eV/Å.

A 9,10-DCA molecule contains three benzene rings and two CN groups (top left in Figure 1). Because of the lone pair in

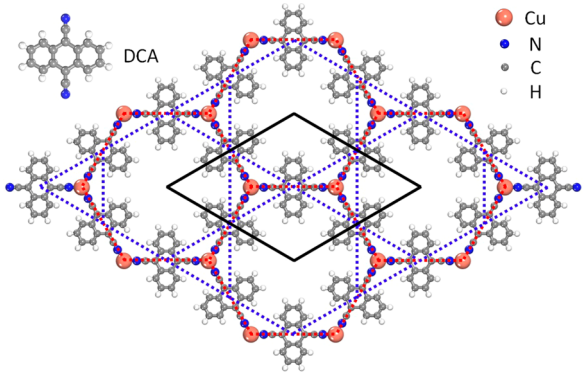

Figure 1. Schematic atomic structure of Cu−DCA film. The top left inset shows the DCA molecule. The red dashed, blue dashed, and black lines outline the honeycomb lattice by the Cu atoms, the Kagome lattice by the DCA molecules, and the unit cell, respectively.

the CN group, this molecule can easily form strong coordination bonds with some transition metal atoms. For example, the linear $Fe(DCA)_2$ and $Ni(DCA)_2$ complexes have been synthesized on the NaCl bilayer on the Cu(111) surface.[26] Recently, two groups have reported the monolayer of Cu−DCA framework growing on Cu(111) surface.[22,23] In Figure 1, we show the optimized freestanding 2D Cu−DCA lattice, which has a hexagonal (honeycomb) lattice formed by the Cu atoms (red dash line), and a Kagome lattice by the DCA molecules (blue dash line).[27] Each Cu atom bonds with three CN groups from the DCA molecules to form a very strong coordination bond (Cu−N bond length is about 1.88 Å). In each unit cell, there are two Cu atoms and three DCA molecules; the optimized lattice constant for the freestanding Cu−DCA lattice is a = 20.36 Å, in good agreement with the experimental results (20.8 ± 0.2 Å) on Cu(111) surface.[23]

Figure 2, panel a shows the band structures and projected density of states (PDOS) of the freestanding Cu−DCA lattice. One sees a typical type of Kagome band around Fermi

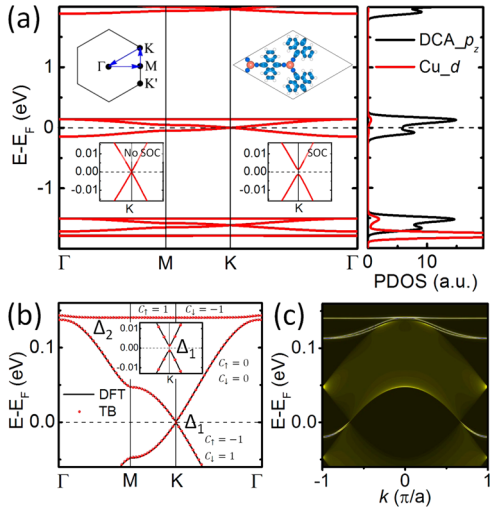

Figure 2. Electronic structures of Cu−DCA film. (a) Band structures and PDOS, where the top right inset indicates the charge distribution around the Fermi level, and the bottom two insets show the zoom-in bands without and with SOC, respectively. (b) The comparison between first-principles and single-orbital TB band structures around two SOC gaps (Δ_1 and Δ_2). (c) The semi-infinite Dirac edge states within the SOC gaps.

level,[10,27,28] consisting of one flat band with a bandwidth of 3.0 meV above two Dirac bands. According to the PDOS, all the Kagome bands mainly come from the p_z-orbital of the DCA molecule, as also indicated by the plot of partial charge density distribution from the Kagome bands (top right inset in Figure 2a), consistent with the Kagome lattice of DCA molecules in Figure 1. Most importantly, different from all the previous Kagome systems studied,[9−16] the Fermi level lies exactly at the Dirac point for the Cu−DCA system. The bottom two insets in Figure 2, panel a show the zoom-in plots without (bottom left) and with SOC (bottom right), respectively. A band gap (Δ_1 = 2.9 meV) opens at the Dirac point after the SOC is included, so that the Fermi level lies exactly inside the SOC gap, indicating the very nature of intrinsic TI states associated with SOC.

We can use the single-orbital TB model on a Kagome lattice[28] to better describe the electronic properties. The corresponding model Hamiltonian is

$$H = \begin{pmatrix} E_0 & 2t\cos k_1 & 2t\cos k_2 \\ 2t\cos k_1 & E_0 & 2t\cos k_3 \\ 2t\cos k_2 & 2t\cos k_3 & E_0 \end{pmatrix} \pm i2\lambda \begin{pmatrix} 0 & \cos k_1 & -\cos k_2 \\ -\cos k_1 & 0 & \cos k_3 \\ \cos k_2 & -\cos k_3 & 0 \end{pmatrix}$$

where $k_1 = (a/2)\hat{x}$, $k_2 = (a/2)[(\hat{x} + \sqrt{3}\hat{y})/2]$,$k_3 = \left(\frac{a}{2}\right)\left[\frac{(-\hat{x}+\sqrt{3}\hat{y})}{2}\right]$, and a is the lattice constant. E_0 is the on-site energy, t is the nearest-neighbor hopping parameter, λ is the nearest-neighbor intrinsic SOC, and ± refers to the spin-up/spin-down bands. The corresponding parameters for the Cu−DCA lattice obtained by fitting with the DFT results are E_0 = 0.0468 eV, t = −0.0468 eV, and λ = 0.00084 eV. Figure 2, panel b shows the excellent agreement between the first-principles (black lines) and single-orbital TB (red dots) band

DOI: 10.1021/acs.nanolett.6b00110
Nano Lett. 2016, 16, 2072−2075

structures around two SOC gaps (Δ_1 = 2.9 meV and Δ_2 = 2.1 meV). Since the Kagome bands around the Fermi level are mainly from the p_z-orbital of the DCA molecule, this molecule can be considered effectively as a superatom. Then the electronic hopping between the DCA molecules in the Kagome lattice is bridged by a Cu atom in between so that the overall SOC strength is enhanced by Cu with the SOC gaps (Δ_1 and Δ_2) significantly larger than that of carbon.

To confirm the topological properties of the Cu−DCA bands, we calculated its Chern number (C=$C_\uparrow + C_\downarrow$) and spin Chern number [$C^s = \frac{1}{2}(C_\uparrow - C_\downarrow)$] for each band with different spins using the Kube formula.[29,30] For the three Kagome bands with both spins around the Fermi level, the flat band and the bottom Dirac band have a nonzero Chern number (±1), while the top Dirac band has a zero Chern number, as marked in Figure 2, panel b. Thus, within the SOC gap (Δ_1 and Δ_2), the Chern number is 0, while the spin Chern number is −1, which indicates that the Cu−DCA lattice is topologically nontrivial. We also calculate the edge states of the Cu−DCA lattice by using the Wannier90 package.[31] To do so, we first fit a TB Hamiltonian in the basis of the maximally localized Wannier functions (MLWFs) to the DFT band structures. Then, using the MLWFs, we construct the edge Green's function of the semi-infinite lattice by using the recursive method[32] and calculate the LDOS of the edge (shown in Figure 2c). From the LDOS, clearly one sees the nontrivial topological edge states that connect with the bulk band edges.

To better understand the intrinsic topological properties of the Cu−DCA lattice, we next perform an electron counting and orbital hybridization analysis. According to the above calculation results, the Kagome bands around the Fermi level mainly come from the p_z-orbital of DCA molecule of the Cu−DCA lattice. In other words, we may consider the DCA molecule as a superatom with two groups of lone pairs in the outer shell, and it tends to accept electrons from its nearest-neighbor Cu atoms (see PDOS of DCA molecule (a) before and (b) after binding with Cu atoms in Figure S1 in the Supporting Information). A schematic drawing of the orbital hybridization between Cu atoms and DCA molecules is shown in Figure 3. The hybridization between d orbitals of Cu atoms

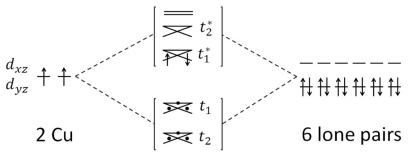

Figure 3. Schematic drawing of the orbital hybridization between Cu atoms and the lone pairs from the CN groups of DCA molecule. Each arrow denotes one electron with an up or down spin, while each black dot denotes two spin-degenerate electrons.

(d_{xz} and d_{yz}) and the lone pairs of CN groups of DCA molecule (π orbitals) leads to four groups of triple states: the bonding states t_1, t_2 and the antibonding states t_1^*, t_2^*. There are a total of 14 valence electrons, two from Cu atoms (other valence electrons of Cu occupy the rest d and s orbitals not involved with hybridization) and 12 from the lone pair of CN groups of DCA molecules. Consequently, t_1 and t_2 bands are fully occupied, leaving another two electrons to fill the bottom half of Dirac bands formed from the t_1^* states so that the Fermi level lies exactly at the Dirac point at K without SOC or inside the SOC gap with SOC. This suggests that similar systems with CN groups and noble metal atoms might also be intrinsic OTIs. Actually, the metal−NC group coordination bonds are very common in the metalorganic frameworks. Many experimental results about the noble metals and transition metals coordinated with CN groups are reported. For example, the two- and three-fold coordination Cu−NC bonds,[22,23,33,34] three-fold coordination Au−NC bonds,[35] three- and four-fold coordination Co−NC bonds,[36,37] two-fold coordination Fe− and Ni−NC bonds,[23] and so on.

Since there are many types of metal−NC group coordination bonds, similar 2D frameworks as the Cu−DCA lattice could also be synthesized. As an example, we have calculated the Au−DCA system by replacing Cu with Au in the Cu−DCA lattice. The optimized lattice constant of Au−DCA is 21.06 Å. In Figure 4, panels a and b, we show its band structures with SOC

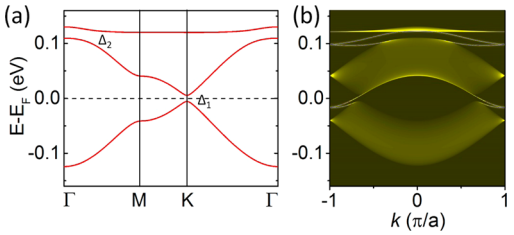

Figure 4. (a) Band structure with SOC and (b) the semi-infinite edge states within the SOC gaps of Au−DCA.

and semi-infinite edge states within the SOC gaps, respectively. The band structures and topology of Au−DCA are found very similar to those of Cu−DCA lattice, except for larger SOC gaps (Δ_1 = 11.3 meV and Δ_2 = 10.6 meV). We also replaced DCA molecule to cyanogens (the smallest molecule with two CN groups) and found that Cu−cyanogen and Au−cyanogen also have the similar band structures and topological properties with those of Cu−DCA, and they are all intrinsic 2D OTIs with larger SOC gaps than Cu−DCA (see Figure S2 and Table S1 in the Supporting Information).

Because of the line properties of CN triple bonds of DCA molecule, the benzene rings in DCA molecule will rotate constantly about the axis connecting the two Cu atoms, but without breaking the bonds (see Figure S3 in the Supporting Information). To quench such rotational freedom and investigate the stability of the Cu−DCA lattice, we also investigate the structure stabilities and electronic properties for Cu−DCA and Au−DCA on h-BN (see Figure S4 and Figure S4 in the Supporting Information) and find that the nontrivial topological properties of these OTIs persist on the h-BN surfaces.

In conclusion, using first-principles calculations, we predict that the Cu−DCA Kagome lattice is an intrinsic 2D OTI. On the basis of electron counting and orbital hybridization analysis, we further predict that similar lattices made of noble metal atoms bonding with molecules containing two CN groups are all intrinsic OTIs. Our findings facilitate the future experimental confirmation of OTIs without the need of doping.

■ ASSOCIATED CONTENT

Supporting Information

The Supporting Information is available free of charge on the ACS Publications website at DOI: 10.1021/acs.nanolett.6b00110.

DOI: 10.1021/acs.nanolett.6b00110
Nano Lett. 2016, 16, 2072−2075

PDOS of DCA molecule and Cu atom in Cu−DCA, schematic atomic structure of Cu−Cyanogen lattice, lattice constants and SOC gap for four metal−molecule lattices, MD simulation of Cu−DCA lattice, relaxed configurations and band structures of Cu−DCA and Au−DCA on *h*BN surface (PDF)

AUTHOR INFORMATION

Corresponding Authors

*E-mail: zhmwang@uestc.edu.cn.
*E-mail: sxdu@iphy.ac.cn.
*E-mail: fliu@eng.utah.edu.

Notes

The authors declare no competing financial interest.

ACKNOWLEDGMENTS

We acknowledge the support of the Natural Science Foundation of China (Nos. 51325204, 61390501, and 51210003), the MOST 973 projects of China (No. 2011CB921702), the Chinese Academy of Sciences (CAS), and Shanghai Supercomputer Center. Z.F.W. and F.L. acknowledge support from DOE-BES (Grant No. DE-FG02-04ER46148).

REFERENCES

(1) Hasan, M. Z.; Kane, C. L. *Rev. Mod. Phys.* **2010**, *82*, 3045.
(2) Qi, X.-L.; Zhang, S.-C. *Rev. Mod. Phys.* **2011**, *83*, 1057.
(3) Kane, C. L.; Mele, E. J. *Phys. Rev. Lett.* **2005**, *95*, 226801.
(4) König, M.; Wiedmann, S.; Brüne, C.; Roth, A.; Buhmann, H.; Molenkamp, L. W.; Qi, X.-L.; Zhang, S.-C. *Science* **2007**, *318*, 766.
(5) Knez, I.; Du, R.-R.; Sullivan, G. *Phys. Rev. Lett.* **2011**, *107*, 136603.
(6) Wang, Z. F.; Liu, Z.; Liu, F. *Nat. Commun.* **2013**, *4*, 1471.
(7) Liu, Z.; Wang, Z. F.; Mei, J. W.; Wu, Y. S.; Liu, F. *Phys. Rev. Lett.* **2013**, *110*, 106804.
(8) Wang, Z. F.; Liu, Z.; Liu, F. *Phys. Rev. Lett.* **2013**, *110*, 196801.
(9) Kambe, T.; Sakamoto, R.; Hoshiko, K.; Takada, K.; Miyachi, M.; Ryu, J.; Sasaki, S.; Kim, J.; Nakazato, K.; Takata, M.; Nishihara, H. *J. Am. Chem. Soc.* **2013**, *135*, 2462.
(10) Sheberla, D.; Sun, L.; Blood-Forsythe, M. A.; Er, S.; Wade, C. R.; Brozek, C. K.; Aspuru-Guzik, A.; Dincă, M. *J. Am. Chem. Soc.* **2014**, *136*, 8859.
(11) Cui, J. S.; Xu, Z. T. *Chem. Commun.* **2014**, *50*, 3986.
(12) Campbell, M. G.; Sheberla, D.; Liu, S. F.; Swager, T. M.; Dincă, M. *Angew. Chem., Int. Ed.* **2015**, *54*, 4349.
(13) Wang, Z. F.; Su, N.; Liu, F. *Nano Lett.* **2013**, *13*, 2842.
(14) Zhou, Q. H.; Wang, J. L.; Chwee, T. S.; Wu, G.; Wang, X. B.; Ye, Q.; Xu, J. W.; Yang, S. W. *Nanoscale* **2015**, *7*, 727.
(15) Zhao, B.; Zhang, J. Y.; Feng, W. X.; Yao, Y. G.; Yang, Z. Q. *Phys. Rev. B: Condens. Matter Mater. Phys.* **2014**, *90*, 201403.
(16) Zhang, X. M.; Zhao, M. W.; Liu, F. *arXiv:1509.06843* **2015**.
(17) Xiong, Z. H.; Wu, D.; Valy Vardeny, Z.; Shi, J. *Nature* **2004**, *427*, 821.
(18) Bogani, L.; Wernsdorfer, W. *Nat. Mater.* **2008**, *7*, 179.
(19) Sanvito, S. *Chem. Soc. Rev.* **2011**, *40*, 3336.
(20) Liu, Z.; Zou, X. L.; Mei, J. W.; Liu, F. *Phys. Rev. B: Condens. Matter Mater. Phys.* **2015**, *92*, 220102.
(21) Kambe, T.; Sakamoto, R.; Kusamoto, T.; Pal, T.; Fukui, N.; Hoshiko, K.; Shimojima, T.; Wang, Z. F.; Hirahara, T.; Ishizaka, K.; Hasegawa, S.; Liu, F.; Nishihara, H. *J. Am. Chem. Soc.* **2014**, *136*, 14357.
(22) Pawin, G.; Wong, K. L.; Kim, D.; Sun, D.; Bartels, L.; Hong, S.; Rahman, T. S.; Carp, R.; Marsella, M. *Angew. Chem., Int. Ed.* **2008**, *47*, 8442.
(23) Zhang, J.; Shchyrba, A.; Nowakowska, S.; Meyer, E.; Jung, T. A.; Muntwiler, M. *Chem. Commun.* **2014**, *50*, 12289.
(24) Kresse, G.; Furthmuller, J. *Phys. Rev. B: Condens. Matter Mater. Phys.* **1996**, *54*, 11169.
(25) Perdew, J. P.; Burke, K.; Ernzerhof, M. *Phys. Rev. Lett.* **1996**, *77*, 3865.
(26) Liljeroth, P.; Swart, I.; Paavilainen, S.; Repp, J.; Meyer, G. *Nano Lett.* **2010**, *10*, 2475.
(27) Zhou, M.; Liu, Z.; Ming, W. M.; Wang, Z. F.; Liu, F. *Phys. Rev. Lett.* **2014**, *113*, 236802.
(28) Tang, E.; Mei, J. W.; Wen, X. G. *Phys. Rev. Lett.* **2011**, *106*, 236802.
(29) Yao, Y. G.; Kleinman, L.; MacDonald, A. H.; Sinova, J.; Jungwirth, T.; Wang, D. S.; Wang, E. G.; Niu, Q. *Phys. Rev. Lett.* **2004**, *92*, 037204.
(30) Yao, Y. G.; Fang, Z. *Phys. Rev. Lett.* **2005**, *95*, 156601.
(31) Mostofi, A. A.; Yates, J. R.; Lee, Y.-S.; Souza, I.; Vanderbilt, D.; Marzari, N. *Comput. Phys. Commun.* **2008**, *178*, 685.
(32) Sancho, M. P. L.; Sancho, J. M. L.; Sancho, J. M. L.; Rubio, J. *J. Phys. F: Met. Phys.* **1985**, *15*, 851.
(33) Pivetta, M.; Pacchioni, G. E.; Schlickum, U.; Barth, J. V.; Brune, H. *Phys. Rev. Lett.* **2013**, *110*, 086102.
(34) Pacchioni, G. E.; Pivetta, M.; Brune, H. *J. Phys. Chem. C* **2015**, *119*, 25442.
(35) Meyer, J.; Nickel, A.; Ohmann, R.; Lokamani; Toher, C.; Ryndyk, D. A.; Garmshausen, Y.; Hecht, S.; Moresco, F.; Cuniberti, G. *Chem. Commun.* **2015**, *51*, 12621.
(36) Schlickum, U.; Decker, R.; Klappenberger, F.; Zoppellaro, G.; Klyatskaya, S.; Ruben, M.; Silanes, I.; Arnau, A.; Kern, K.; Brune, H.; Barth, J. V. *Nano Lett.* **2007**, *7*, 3813.
(37) Stepanow, S.; Lin, N.; Payer, D.; Schlickum, U.; Klappenberger, F.; Zoppellaro, G.; Ruben, M.; Brune, H.; Barth, J. V.; Kern, K. *Angew. Chem., Int. Ed.* **2007**, *46*, 710.

DOI: 10.1021/acs.nanolett.6b00110
Nano Lett. 2016, 16, 2072−2075